Effect of step stiffness and diffusion anisotropy on dynamics of vicinal surfaces: A competing growth process

M. Guedda,[1,*] H. Trojette,[1] S. Peponas,[1,2] and M. Benlahsen[2]
[1]*LAMFA, CNRS UMR 6140, Department of Mathematics, Université de Picardie Jules Verne, 33 Rue Saint-Leu, Amiens, France*
[2]*LPMC, Department of Physic, Université de Picardie Jules Verne, 33 Rue Saint-Leu, Amiens, France*
(Received 26 October 2009; revised manuscript received 30 March 2010; published 26 May 2010)

We re-examine the step meandering instability which is described in term of solutions to the Conserved Kuramoto-Sivashinsky (CKS) equation [Frisch and Verga, Phys. Rev. Lett. **96**, 166104 (2006)]. A free-boundary approach is used to exhibit a class of exact solutions that may give a reasonable description of the observed characteristic features of the instability. Different scenarios are found: the characteristic lateral coarsening (i) grows with time like $\sqrt{t}$ (typical behavior), (ii) disappears, (iii) or does not change for all time (localization in space), depending on the initial transverse meandering amplitude k_0, or the initial typical height. Those regimes are compared by the numerical simulations presented in the literature. For case (ii) the collapsing time is expressed as an algebraic function of k_0.

DOI: 10.1103/PhysRevB.81.195436 PACS number(s): 81.15.Hi, 47.20.Hw, 68.35.Ct, 81.10.Aj

I. INTRODUCTION

Molecular beam epitaxy (MBE), which has many important technological and industrial applications, is often used to grow nanostructure on crystal surfaces. Under nonequilibrium growth a very rich variety of crystal surface morphologies[1] are experimentally observed resulting from nonlinear evolution of step branching[2,3] and meandering instabilities.[4–6] A major goal in nonequilibrium physics is to predict the behavior of surface evolution from the knowledge initial arbitrary profile. Near the instability threshold meander evolution can often, in principle, be described by simple nonlinear amplitude equations having universal form.

Recently, Frisch and Verga[7,8] studied the step meandering instability on a surface characterized by the alteration of terraces with different properties as in the case of Si(001). Under the assumption of negligible desorption and Ehrlich-Schwoebel the surface morphology is investigated by means of the following unstable mode equation (Conserved Kuramoto-Sivashinsky, CKS for short):

$$\partial_t u = -\partial_y^2\left[\frac{f\alpha}{48}(f\alpha+12\delta)u+\partial_y^2 u+\frac{f}{12}(\partial_y u)^2\right], \qquad (1)$$

or after scaling,

$$\partial_t u = -\partial_y^2\left[u+\partial_y^2 u+\frac{1}{2}(\partial_y u)^2\right]. \qquad (2)$$

Such equation has been used to describe a variety of mechanisms (see below). In the regime of interest here, the unknown function $u(y,t)$ designates the amplitude of the unstable branch and y and t represent the coordinate along the step and time. The first linear term on the right-hand side of Eq. (1) is the instability term. This term is balanced by the classical stabilizing linear term à la Mullins. The nonlinear term is responsible of the coarsening dynamics, i.e., the amplitude and lateral width increase with time without bound. To derive the CKS equation from the Bales-Zangwill (BZ) instability[4] a multiscale analysis is performed by introduced the slow temporal and spacial variables $\varepsilon^6 t \to t, \varepsilon y \to y$, where the parameter ε represents the distance to the threshold. In the CKS equation the parameters f, α and δ are given by

$$f_0 = \varepsilon f, \quad \delta_0 = \varepsilon\delta, \quad \alpha_0 = 1+\varepsilon^2\alpha, \qquad (3)$$

with the physical parameters $f_0>0$, $\alpha_0>1$, and δ_0 referring to the flux parameter, ratio of diffusion anisotropy coefficients and step stiffness difference parameter, respectively. The authors founded that the instability appears above a flux threshold $f_0>f_{0c}$, where $f_{0c}=-12\alpha_0\delta_0/(\alpha_0-1)$ and $f_0>0$.[7]

The purpose of this article is to study different dynamical behaviors, in mathematical terms that may result from Eq. (1). Examination of the linear dispersion relation

$$\omega = \frac{f\alpha}{48}(f\alpha+12\delta)q^2-q^4, \qquad (4)$$

where ω is the linear amplification rate and q is the wave number, showed that, for positive values of $f\alpha+12\delta$, there exists a critical wavelength, $\lambda_c=\frac{8\pi\sqrt{3}}{\sqrt{f\alpha(f\alpha+12\delta)}}$, that separates unstable steps from stable ones. The wavelength λ_m of the most unstable mode is $\lambda_m=\sqrt{2}\lambda_c$ (obtained from $\partial_q\omega=0$). The instability develops after a finite time (the typical time for the instability) of the order t_u given by

$$t_u = \frac{96^2\varepsilon^{12}}{\{f_0(\alpha_0-1)[f_0(\alpha_0-1)-12\varepsilon^2\delta_0]\}^2}. \qquad (5)$$

II. FORMULATION OF THE PROBLEM

The CKS Eq. (1) can be viewed as a standard model which arises in various physical situations. If desorption is negligible, it was mentioned that Eq. (1) is a possible (natural) candidate for the time-evolution of the meandering amplitude.[11] In the context of amorphous thin film growth this equation has been studied as the minimal deterministic deposition equation.[9] Equation (2) can be interpreted as a particular case of the following modified CSK equation

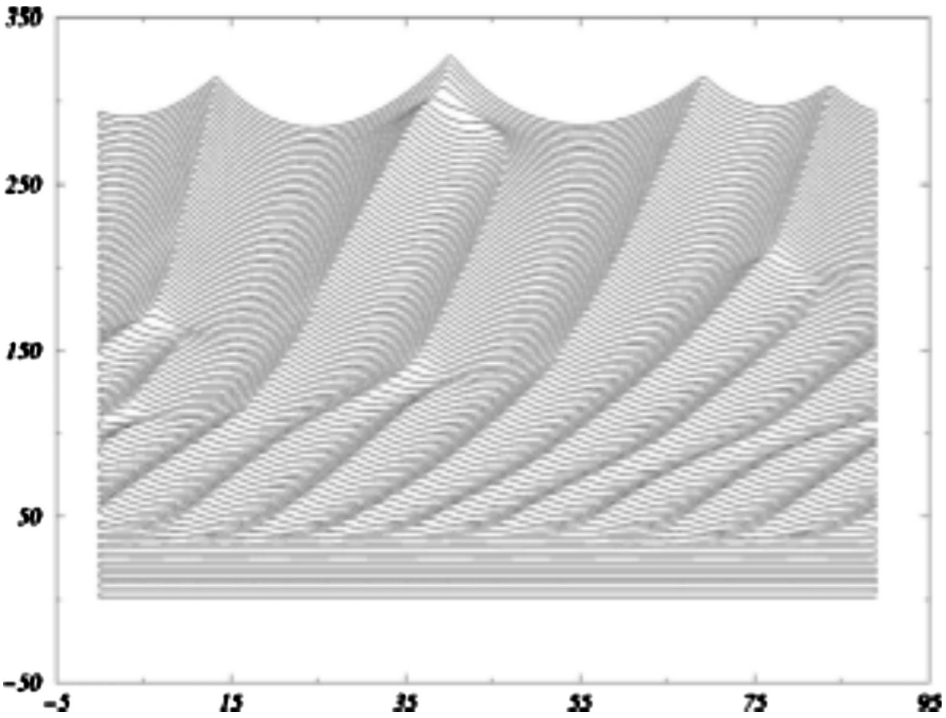

FIG. 1. Numerical solution of the modified CKS Eq. (6) with $\gamma=1$ according to Ref. 6.

$$\partial_t u = -\partial_y^2\left[u - \gamma\partial_y u + \partial_y^2 u + \frac{1}{2}(\partial_y u)^2\right]. \tag{6}$$

This partial differential equation (PDE) has been derived in model of bunches created by an electromigration current.[6] Equation (6) was also proposed to represent sand ripples formation close to the instability threshold.[12] In the present physical context the term $\partial_y^3 u$ leading to a dispersive drift must be absent. It is worth noticing that this term can be removed from Eq. (6) via transformation $u \to u - \gamma y$. More recently, Politi and ben-Avraham[13] showed that the CSK equation can be mapped into the motion of a system of particles with attractive interactions, decaying as the inverse of their distance. The CKS equation is a closely related more general equation,

$$\partial_t u = -\partial_y^2[u + \partial_y^2 u + \gamma(\partial_y u)^2] + \Gamma(\partial_y u)^2, \tag{7}$$

where γ and Γ are real (physical) parameters. This equation appears in the context of ion beam sputtering.[15] The above equation was also proposed for amorphous thin films in the presence of potential density variations.[16] Equation (7) also referred to as the snow equation. Under the condition $\gamma^2 + \Gamma^2 = 1$, this equation models a snow surface growth based on solar radiation.[17] In this example the unknown u denotes the surface height of snow relative to a horizontal reference plane. The equation is proposed by Tiedje *et al.*, in two-dimensional case, to explain the dynamical behavior of the ablation hollows or sun cups in terms of the interaction of solar radiation with the snowpack.

Very recently, Verga[18] investigated the influence of the vicinal surfaces anisotropy on the two-dimensional dynamics of the meandering instability. In this case the continuum model reads, for some physical positive parameters A, B, and C,

$$\partial_t u = -\partial_x^4 u - A\partial_x^3 u - \partial_y^2[u + \partial_y^2 u + (\partial_y u)^2 + B\partial_x u + C\partial_x^2 u]. \tag{8}$$

Our motivation in the CSK equation stems from an unified result, presented in Refs. 6, 9, 11, and 15 to describe the coarsening dynamics. It is shown that the characteristic length scale of the surface structure and its typical height grow as $\sqrt{t}$ and t, respectively. Moreover, it is found that this coarsening has the property that small mounds or cells disappear at the benefit of larger neighbors (Fig. 1). This phenomenon has been also observed in Ref. 14. In Ref. 16 the authors concluded that, for Eq. (7) with γ and Γ being positive, small mounds vanish and larger mounds grow at the expense of their smaller neighbors, until they split into smaller mounds, while in the absence of the term proportional to Γ (the CKS equation) the large mounds do not spilt. For the two-dimensional problem [Eq. (8)] Verga showed, by a numerical study, that the amplitude grows linearly with time and that the characteristic lengths λ_x and λ_y, along both directions (perpendicular and parallel to the steps), vary as t^{n_x} and t^{n_y} for large t, respectively, where $n_x=0.25$ and $n_y=0.52$. In addition, it is observed that the dynamic in the y direction (meander) is similar to the dynamic described by the CKS equation. Note that Eq. (8) may admit an additive separable solution $u(x,y,t)=u_1(x,t)+u_2(y,t)$, where u_1 is a solution to $\partial_t u=-\partial_x^4 u-A\partial_x^3 u$ and u_2 is a solution to an equation of the form Eq. (2).

Despite the different physical context, the previous results cannot be excluded *a priori* for the step meandering instability on Si(001) surface. To explore analytically the effect of the step stiffness and diffusion anisotropy on the instability regime, a nonlinear analysis is reported in Ref. 7. Using a simplified equation [see Eq. (13) below] the authors obtained a $t^{1/2}$ scaling, for large time, and also demonstrated a linear

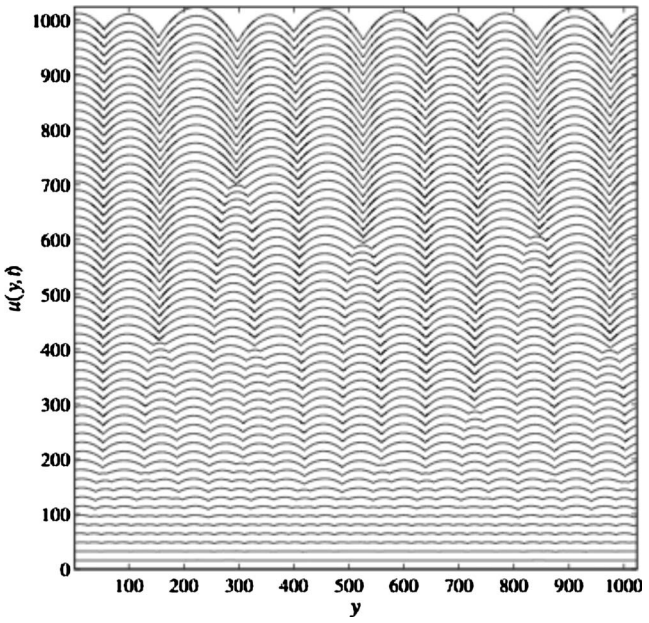

FIG. 2. Numerical solution of the full CKS equation given in Fig. 3 of Ref. 7. This shows the step profile evolution in the course of time, starting from a random profile. Solutions with small mound disappear at the benefit of larger ones (Ref. 6) [bigger parabolas eat neighboring smaller ones (Ref. 13)]. Observe that (after $t=100$) the collapsing time is proportional to the lateral characteristic.

time growth of the characteristic meander amplitude, in partial accordance with numerical treatments (see below). However, a limitation of these studies, for a mathematical point of view, is that the fourth-order derivative term in CKS equation is assumed to be negligible for the theoretical analysis. Consequently, one class of pattern formation was privileged. A numerical comparison with the analytical results was also attempted.[7] The full Eq. (1), subject to an initial random condition, was numerically integrated. Two different classes of numerical solutions are clearly observed (see Fig. 2 or 3 of Ref. 7). The first class has the typical behavior; i.e., the characteristic length scale and the amplitude grow as $\sqrt{t}$ and t, respectively, while the second one disappears at a finite time. It is this last possibility that prompted the present investigation. Our aim here is not to introduce another intuitive or speculative physical scenario. Rather, an effort is made to exhibit analytically important qualitative features of the CKS equation being observed in numerical simulations. Without entering into the detail, a simple inspection of Fig. 3 of Ref. 7 allows us to conclude naively that any solution with small mound, or with small initial transverse amplitude meandering, will disappear at a finite time. Even without experiment results, we are convinced that the above scenarios cannot be excluded by any physical argument. Since we regard these properties as physically relevant, the goal of the present paper is to re-examine the CKS equation incorporating surface diffusion. In this study we present the free-boundary approach introduced in Ref. 7. We find that the interplay of the instability term, Mullins and the nonlinear terms gives rise to a complex behavior, in which the several distinct physical mechanisms can be described in terms of a simple nonlinear ordinary differential equation (ODE).

III. MOVING-BOUNDARY APPROACH

From the theoretical point of view the major interest of the CSK equation lies in the competition between the growth instability inherent in the step stiffness and diffusion anisotropy and the stabilizing influence of the surface diffusion. In improvement on the studies of Ref. 7, here the Mullins term u_{yyyy}, is not neglected. This term will turn out to be decisive for the stability via the moving-boundary approach. It is one of novelties of this paper to report on an analytical justification of the existence of meanders which correspond to, or predict, a finite collapsing time (or a singularity). General criteria for different dynamical scenarios are derived. We shall discuss the occurrence of the finite collapsing-time, which is in general associated with the "smallest" initial data. In particular, we shall obtain an explicit expression for the finite collapsing time, and this is probably due to the presence of the stabilizing term. We further study the effect of parameters f, α, and δ on the time evolution of the meander. So far, no theoretical classification of the step meandering instability has been established. This is useful for interpreting some experiments and for verifying more complicated numerical schemata. Our result may give some light to the perspective pointed out by Gillet *et al.* in Ref. 6 for Eq. (6).

A. Similarity profile

As a first approach to extract the coarsening behavior, one commonly uses the scaling argument or the invariance property. The analysis presented in the present discussion has followed, with slight modification, the approach of Frisch and Verga. The starting point is to look for a similarity solution to the CKS equation. Using the scaling ansatz

$$u_s(y,t) = t^a \varphi(\eta), \quad \eta = y t^{-b} \tag{9}$$

we deduce from Eq. (1) that $a=1$, $b=\frac{1}{2}$. The profile φ satisfies

$$\frac{1}{t}\varphi^{(iv)} + \frac{f}{12}(\varphi'^2)'' + \frac{f\alpha}{48}(f\alpha + 12\delta)\varphi'' - \frac{1}{2}\eta\varphi' + \varphi = 0, \tag{10}$$

where the prime denote differentiation with respect to η. However, the above equation is not an ODE for φ. At the first sight, the Mullins term u_{yyyy} destroys the similarity structure in the sense that the PDE cannot be reduced to an ODE. We may deduce, *a priori*, that the coarsening process of Eq. (1) cannot inferred from a scaling argument. In the present context, it is mentioned in Ref. 9 that the invariance property is fulfilled only if we neglect one of the three terms on the rhs of the CKS equation. In fact, the only way to have similarity solution (9) is to impose $\varphi^{(iv)} \equiv 0$. Together with Eq. (10) we infer that the shape function is given explicitly,

$$\varphi(\eta) = v_0 - \rho\eta^2, \tag{11}$$

where ρ is an undetermined constant and $v_0 = -\frac{2f}{3}\rho^2 + \frac{f\alpha(f\alpha+12\delta)}{24}\rho$. Using expression (11) in relation (9) we get immediately

$$u_s(y,t) = v_0 t - \rho y^2, \tag{12}$$

which is the famous Ivantsov-type solution, for positive v_0 and ρ.[10] Remarkably, the explicit solution u_s is the unique similarity solution to the CKS equation in the usual form Eq. (9) for $v_0 \neq 0$; i.e., $u_s(y,t) = t(v_0 - \rho\eta^2)$.

Assuming that the Mullins term is negligible the CKS equation reads

$$\partial_t u = -\partial_y^2 \left[\frac{f\alpha}{48}(f\alpha + 12\delta)u + \frac{f}{12}(\partial_y u)^2 \right]. \tag{13}$$

Mathematically, this assumption is less innocuous than it may seem. As a consequence, the simplified Eq. (13) validates the naive application of the scaling argument.[7,9] In this case the similarity structure, Eq. (9) becomes exact for any $t>0$, and the profile φ satisfies the following degenerate ODE:

$$\frac{f}{12}(\varphi'^2)'' + \frac{f\alpha}{48}(f\alpha + 12\delta)\varphi'' - \frac{1}{2}\eta\varphi' + \varphi = 0. \tag{14}$$

Clearly, the above ODE admits the exact solution

$$\varphi_0(\eta) = -\frac{\alpha(f\alpha + 12\delta)}{16}\eta^2, \tag{15}$$

which leads to an exact solution for both Eqs. (13) and (1) in the form of a stationary parabola $[v_0=0,\ \rho=\alpha(f\alpha+12\delta)/16]$ (Refs. 7 and 9),

$$u(y,t) = -\frac{\alpha(f\alpha + 12\delta)}{16}y^2. \tag{16}$$

Finally, similar to the situation for dendritic growth,[10] numerical solutions of Ref. 7 showed that the general asymptotic solutions can be thought as a superposition of parabolas (Ivantsov solution) of the form Eq. (16) (see Refs. 7 and 9). In Ref. 5 it is mentioned that the function of the form Eq. (16) can be considered as an approximation of solutions to Eq. (7) for large values of γ, or small values of Γ.

B. Different scenarios: The effect of the relaxation term

To elucidate the effects of the physical parameters and the stabilizing term, an analytical analysis will be executed. In order to avoid technical complication, the idea is to study the (short and long-time) dynamics emerging from an initial condition which is a parabola of the form Eq. (16) and localized in space. Following Ref. 7 as a key to the understanding of the competing growth process, we shall be interested in a solution u to Eq. (1) satisfying

$$u(y,t) = -\frac{\alpha(f\alpha + 12\delta)}{16}y^2\chi_t(y), \tag{17}$$

representing a single "mound," where χ_t is the characteristic function of the interval $[y_-(t), y_+(t)]$, where the interfaces, or parabola edges, y_- (left "front") and y_+ (right "front") are unknown functions which are to be determined. Note that since Eq. (1) is invariant under the $y \to -y$ symmetry, we shall assume, without any essential physical changes, $-y_-(t) = y_+(t) = y_0(t)$. Expression (17) assumes that the initial step amplitude $u(y,0)$ is given, for some positive $k_0 = y_0(0)$, by the truncated parabola

$$u(y,0) = -\frac{\alpha(f\alpha + 12\delta)}{16}y^2 \quad \text{for} \quad |y| < k_0, \tag{18}$$

and zero elsewhere. Clearly, the parabola edge involves both the characteristic lateral width $[\lambda(t) \sim y_0(t)]$ and the characteristic meander amplitude of u (defined as $A = \max_y u - \min_y u$) $A(t) = A(0)k_0^{-2}y_0^2(t)$, where the initial characteristic meander amplitude $A(0) = \frac{\alpha(f\alpha+12\delta)k_0^2}{16}$.

The basic property that reduces Eq. (1) to a moving-boundary problem is that the second-order moment for any rapidly decreasing solution to the full equation satisfies [see Eq. (14) of Ref. 7]

$$\frac{d}{dt}\frac{1}{2}\int u^2 dy = \frac{f\alpha}{48}(f\alpha + 12\delta)\int (\partial_y u)^2 dy - \int (\partial_y^2 u)^2 dy. \tag{19}$$

The parabola edge $y_0(t)$ will be computed from identity (19). This allows to determine the coarsening process for Eq. (1). As mentioned in Ref. 7, identity (19) shows that the amplitude of u tends to increase in regions where the gradient term dominates the term $\partial_{yy}u$. It turns out that the above identities will play a crucial role in the time behavior of solutions. In particular, we shall see how the relaxation term acts on the short and long time of the characteristic lateral width. Physically, Eq. (19) indicates that a competition between the step stiffness, diffusion anisotropy effect and the stabilizing is not ineffective. Here, we shall see that Eq. (19) has a nontrivial fixed point which is unstable. At this point, we would like to stress that identity (19) still holds even if $\gamma\partial_y^3 u$ is present.

In order to study different scenarios which can be reached from the initial transverse meandering amplitude one should consider Eqs. (17) and (19) simultaneously. In that event, we find that the free boundary or the parabola edge can be obtained as the unique solution of the equation

$$y_0^4 \frac{d}{dt}y_0(t) = \frac{f\alpha}{18}(f\alpha + 12\delta)y_0^3(t) - 8y_0(t), \tag{20}$$

starting initially from the width $k_0 \geq 0$, i.e.,

$$y_0(0) = k_0. \tag{21}$$

Beyond the numerical results reported in the literature, mathematically, one may ask what kind of behavior can occur with different conditions on the initial data k_0. Here it is required that $f\alpha + 12\delta > 0$ (large diffusion anisotropy accompanied with small step stiffness difference) which is plainly satisfied if ε^2 is small enough. The main question we address in this work is the degree to which the physical properties of the full equation can be systematically derived from the above free-boundary problem.

For a useful comparison, we first consider the case where the term u_{yyyy} is absent. In such a case the parabola edge satisfies[7]

$$y_0^4 \frac{d}{dt} y_0(t) = \frac{f\alpha}{18}(f\alpha + 12\delta) y_0^3(t).$$

This leads to the following explicit expression for y_0:

$$y_0(t) = \sqrt{\frac{f\alpha}{9}(f\alpha + 12\delta)t + k_0^2}. \tag{22}$$

Then one obtains that the solution (17) can be written in the similarity form [Eq. (9)]. Clearly, the amplitude of the meander still increases as t and the lateral width grows as $\sqrt{t}$, irrespective of $k_0 \geq 0$. However, the scaling form [Eq. (9)] is not compatible with identity (19), in particular, for short t. The time derivative and the first term of the right-hand side increase as $t^{3/2}$, while the last term increases as $t^{1/2}$. So, it may be necessary to consider solutions of the type [Eq. (17)] satisfying identity (19) for all $t \geq 0$. This may permit a more refined analytical description of properties of solutions to the CKS equation.

To reinforce the effect of the term u_{yyyy}, via the free-boundary approach, we investigate briefly, the following equation:

$$\partial_t u = -\partial_y^2[\partial_y^2 u + a(\partial_y u)^2], \tag{23}$$

where $a = \frac{f}{12}$. This equation is known as the deterministic Lai-Das Sarma-Villain (LDV) equation or the conserved Kardar-Parisi-Zhang equation for appropriate parameter a. In this limit identity (19) reads

$$\frac{d}{dt}\frac{1}{2}\int u^2 dy = -\int (\partial_y^2 u)^2 dy,$$

showing that the amplitude of u decreases as t increases, irrespective of a. This may explain why some numerical solutions to the full equation disappear at a finite time.

In the remainder we will theoretically report on the classification of solutions and the effect of the physical parameters f, α, and δ for the full amplitude Eq. (1). This probably affords best physical insights. Four situations will be addressed.

1. Typical behavior (noninterrupted coarsening)

Under "typical" we mean that the lateral meander width has the power-law dependance on (large) t. For the present purpose we define the (critical) width

$$k_c = \frac{12}{\sqrt{f\alpha(f\alpha + 12\delta)}} = \frac{\sqrt{6}}{4\pi}\lambda_m. \tag{24}$$

The expression of k_c corresponds to the positive equilibrium point of Eq. (20). We will study how k_0 does determine the growth process. We can understood, as anticipated, that the dynamics for $k_0 > k_c$ and for $k_0 < k_c$ can be completely different. Note that if the parabola edge y_0 exists our exact solution (17) will move, in the course of time, with (tip) velocity (along the x-axis direction),

$$v(t) = \frac{\alpha(f\alpha + 12\delta)}{144}\left[f\alpha(f\alpha + 12\delta) - \frac{144}{y_0^2(t)}\right]. \tag{25}$$

Let us return to the free-boundary problem. For $k_0 > k_c$ we find that the (unique) solution y_0 to Eqs. (20) and (21), is given in the implicit form

$$y_0^2(t) + k_c^2 \ln\left(\frac{y_0^2(t) - k_c^2}{k_0^2 - k_c^2}\right) = \frac{f\alpha}{9}(f\alpha + 12\delta)t + k_0^2. \tag{26}$$

Using the above algebraic equation one can see that $y_0(t)$ follows asymptotically a $\sqrt{t}$ behavior (for any $k_0 > k_c$). In this way we can understood the result of Frisch and Verga, which suggests that the dynamics of large amplitude smooth region of u is almost independent of the stabilizing term. To be more precise Eq. (26) leads to the asymptotic behavior

$$y_0^2(t) \sim \frac{f\alpha}{9}(f\alpha + 12\delta)t - k_c^2 \ln(t), \tag{27}$$

as t tends to infinity [see also Eq. (22)], which is the desired typical behavior. Therefore, the amplitude of u grows (linearly), for t large, with the slope

$$\frac{dA}{dt} \sim \frac{f\alpha^2(f\alpha + 12\delta)^2}{144} - \frac{9}{ft}. \tag{28}$$

More interesting is the behavior of $y_0(t)$ for short t. Numerical simulations of Eq. (8), presented in Ref. 18 indicated that the characteristic lengths are convex for small t and concave for large t. In simple words, we shall also investigate the effect of the initial distribution, or the initial transverse meandering amplitude, on the geometrical properties of the parabola edge. Since the second derivative of the parabola edge satisfies

$$y_0'' = \frac{8}{y_0^7 k_c^2}(k_e^2 - y_0^2)(y_0^2 - k_c^2), \tag{29}$$

where $k_e = \sqrt{3}k_c$, we deduce for $k_c < k_0 < k_e$ that there exists a time t_1 such that the curve of y_0 is changed from convex into concave and remains concave after t_1. t_1 is the time when y_0 reaches k_e, and is it determined analytically from Eq. (26),

$$t_1 = \frac{9}{f\alpha(f\alpha + 12\delta)}\left[3k_c^2 - k_0^2 + k_c^2 \ln\left(\frac{2k_c^2}{k_0^2 - k_c^2}\right)\right]. \tag{30}$$

Obviously, for $k_c \geq k_e$ the curve of the parabola edge remains concave for all $t \geq 0$. Similar geometrical properties are obtained numerically in Refs. 6 and 9 for different physical contexts.

Those results agree with the numerical solutions (for large t) presented in Ref. 7 and 6 and also with the analytical results presented in Ref. 9 for mound like surface structures. Note that the long-time behaviors of the parabola edge and the amplitude are not influenced by the initial transverse meandering amplitude, nor by the relaxation term. As mentioned in Ref. 9 we can note here that the asymptotic behavior of the parabola edge does not depend on the nonlinear term of the CKS equation. Estimate Eq. (27) becomes exact; $y_0(t) = \sqrt{\frac{f\alpha}{9}(f\alpha + 12\delta)t}$, in a limit where the relaxation term in the CKS equation is absent [see Eq. (22)]. This proves that

for an initially imposed transverse meandering $k_0 > k_c$ the long-time dynamic is controlled by the instability term. Hence, the relaxation term can be neglected for large t and then the dynamic exhibits a self-similarity regime. For small t, it will be better to underline the difference between the CKS equation and its simplified model. The dynamic is controlled not only by the instability term, but also by the relaxation term. A global picture appeared reasonably correct by comparing with the results of other physical situations. The mechanism of the surface growth seems to make a major contribution to this process. The present trend can be connected to the diffusive motion of adatoms on vicinal surfaces. The surface nonequilibrium current has the same direction as the slope and consequently tends to increase the local slope. The amplitude grows, without limit, by the instability term preferentially in regions of strong gradient.

Alternatively, we shall see in the next result that the surface shape changes qualitatively for small k_0. Although the present scenario is mathematically correct, a saturation of the amplitude at long times can be produced by a possible release of elastic strain energy stored in the layer and described by nonlinear terms that are not included in the CKS equation. In Ref. 11 the authors indicated that possible candidates for amplitude saturations are the strong anisotropy and elastic step interactions.

2. Extinction at finite time

The second situation is that where the initial width takes place in the interval $(0,k_c)$. We shall see that the CKS equation shares analytically another property. Namely, we shall see that $u(y,t)=0$, or $u(y,t)=$const., for any y and any $t \geq t_c$, for some $t_c > 0$. This leads to an ideal vicinal growth. This is precisely what one would physically expect for small "mounds." This conclusion is consistent with the numerical solutions obtained in Fig. 2 (see Refs. 6 and 7). This second property can be obtained simply by analyzing the sign of the first derivative of y_0. From Eq. (20) one sees that the solution y_0 decreases as long as $y_0 < k_c$ and reaches zero at a finite time. This dynamic forces u to collapse. It is of interest to estimate the characteristic time (collapsing time) needed for the rescaled step shape to disappear. The collapsing time t_c is defined as the zero of y_0. According to Eq. (26), t_c is given by

$$t_c = \frac{9}{f\alpha(f\alpha + 12\delta)}\left[k_c^2 \ln\left(\frac{k_c^2}{k_c^2 - k_0^2}\right) - k_0^2\right]. \tag{31}$$

The above equation can be used as a way to estimate, for a given collapsing time, the initial width which is determined as the root of Eq. (31). This useful equation also shows that t_c increases for increasing k_0, tends to infinity if k_0 approaches k_c and t_c approaches 0 with k_0. It can be verified that the profiles of the parabola edge and the amplitude of u at $t=t_c$ are given by

$$y_0(t) \sim 2^{5/4}(t_c - t)^{1/4}, \quad A(t) \sim \frac{\sqrt{2}}{4}\alpha(f\alpha + 12\delta)\sqrt{t_c - t},$$

as $t \to t_c^-$.

In order to make a quantitative comparison of the collapsing time with the typical time of the instability, we need to evaluate Eq. (31) as a function of the ratio k_0/k_c. Setting $k_0 = \tau k_c$, where $\tau \in (0,1)$, the collapsing time can be expressed in physical variables

$$t_c = \frac{9\varepsilon^6 k_c^2}{f_0(\alpha_0 - 1)[f_0(\alpha_0 - 1) + 12\varepsilon^2\delta_0]}\left[\ln\left(\frac{1}{1-\tau^2}\right) - \tau^2\right], \tag{32}$$

where

$$k_c = \frac{12\varepsilon^3}{\sqrt{f_0(\alpha_0 - 1)[f_0(\alpha_0 - 1) + 12\varepsilon^2\delta_0]}}.$$

Combining Eqs. (3) and (24) it is verified that

$$t_c \sim \varepsilon^{12}\left(\frac{6}{f_0(\alpha_0 - 1)}\right)^4\left[\ln\left(\frac{1}{1-\tau^2}\right) - \tau^2\right], \quad k_c \sim \frac{12\varepsilon^3}{f_0(\alpha_0 - 1)},$$

as $\varepsilon \to 0$, showing the dependence of t_c on the flux and diffusion anisotropy. Note that the above estimates are exact for $\delta_0 = 0$ (no difference between step stiffness). Equation (31) predicts that the collapsing time is almost vanishing for large $f_0(\alpha_0 - 1)$. From Eq. (32) it clearly appears that

$$\frac{t_c}{t_u} = \left(\frac{3}{8}\right)^2\left[\ln\left(\frac{1}{1-\tau^2}\right) - \tau^2\right] = \rho(\tau),$$

where t_u is the typical time for the instability [see Eq. (5)]. The ratio ρ maps the interval (0,1) onto the interval $(0,\infty)$. This seems paradoxical since $\frac{t_c}{t_u} \gg 1$, on $(\tau_0,1)$ for some $0 < \tau_0 < 1$. This means that the collapsing time is longer than the typical instability time for $\tau > \tau_0$. The incorporation of the Mullins term in the course of the analysis, may explain why, in the coarsening process, smaller surface heights or mounds are eaten by their bigger neighbors.

3. Localization in space (nonmoving front)

We now turn to the case where y_0 takes initially the critical width k_c. Clearly, we get $y_0(t) = k_c$ for all $t \geq 0$. Therefore

$$u(y,t) = -\frac{\alpha(f\alpha + 12\delta)}{16}y^2\chi(y),$$

where χ is the characteristic function of the interval $(-k_c,k_c)$. This indicates, in particular, that the CSK equation admits a steady-state periodic profile

$$u_s(y,t) = \frac{\alpha(f\alpha + 12\delta)}{16}[k_c^2 - y^2], \quad |y| \leq k_c, \tag{33}$$

with the spatial periodicity $\lambda_s = \frac{\sqrt{3}}{\vartheta}\lambda_c$. The (fixed) amplitude of the oscillation is given by $A = \frac{\vartheta}{8f}$. This pattern has the property that the second-order moment of the local slop is identical to the second order moment of $\partial_{yy}u$,

$$\frac{f\alpha}{48}(f\alpha + 12\delta)\int_{|y|<k_c}(\partial_y u)^2 dy = \int_{|y|<k_c}(\partial_y^2 u)^2 dy.$$

The present result predicts that there is only one family of periodic parabolic stationary solution with the wavelength

frozen at λ_s. It turns out that this stationary solution is unstable. Since, as stated above, for an arbitrary small deviation of k_0 from k_c, the amplitude increases without limit or collapses.

4. Exponential decay

Guided by the above steady state we examine, as a final scenario, the free-boundary problem associated to

$$u(y,t) = \frac{\alpha(f\alpha + 12\delta)}{16}(\Lambda^2 - y^2)\chi_t(y), \tag{34}$$

where $\Lambda > 0$ is a real number and the function χ_t is defined in Eq. (17). In this case we shall see unexpectedly that, under some initial condition, the amplitude and the characteristic wavelength decrease exponentially with time.

The same argument applies to Eq. (34) so that we are left with solving the following initial value problem

$$(\Lambda^2 - y_0^2)^2 \frac{d}{dt} y_0 = \frac{f\alpha}{18}(f\alpha + 12\delta) y_0 (y_0^2 - k_c^2),$$

$$y_0(0) = \Lambda. \tag{35}$$

When $\Lambda = 0$ Eq. (35) is simply the initial value problem [Eqs. (20) and (21)]. Arguing as above we may deduce, as expected, that if $\Lambda > k_c$ problem [Eq. (35)] has the typical behavior, while for $\Lambda = k_c$ one sees that $y_0 \equiv k_c$. Hence, relation (33) holds. For $\Lambda < k_c$ the amplitude computed from Eq. (35) collapses at long times. In addition, a simple analysis shows that, as t tends to infinity, $y_0(t)$ behaves like

$$y_0(t) \sim e^{-8/\Lambda^4 t}, \tag{36}$$

and the amplitude of the meander behaves like $\frac{\alpha(f\alpha+12\delta)}{16} e^{-(16/\Lambda^4)t}$. Finally, let us note that $y_0'(t)$ is unbounded as t approaches the origin for any $\Lambda \neq k_c$.

For completeness, we end our analysis by noting that the method, described above, applies also for negative values of $f\alpha + 12\delta$. Not surprisingly, the solution (17) vanishes at a finite time for any arbitrary initial width $k_0 > 0$ (see the stability diagram in the plane (f_0, δ_0) given in Ref. 7 for $\alpha_0 > 0$). The collapsing time is given by

$$t_c^\star = \frac{9}{|f\alpha(f\alpha + 12\delta)|}\left[k_c^2 \ln\left(\frac{k_c^2}{k_c^2 + k_0^2}\right) + k_0^2\right]. \tag{37}$$

IV. CONCLUSION

In this paper we have aimed to use the free-boundary approach of Frisch and Verga that allows us to exhibit a unified description emerging from the CKS equation. A central part of the present work is the derivation of a class of exact solutions which describe different behaviors actually being observed in numerical simulations.

Using a parabolalike structure the CKS equation was reduced to a simple time nonlinear ODE. This equation, containing the driving instability term which competes with the relaxation term, allows a reliable meander description. In complementarity of Ref. 7, the present work gives an alternative choice of different behaviors, which may explain the complex step structures observed in Si(001) epitaxial growth.

At the first sight, our results can be hampered by the limited range of the initial condition (18) and the truncated parabola expression of solutions. Nevertheless, in addition to the Ivantsov-type solutions, it is reported that the general solution to the CKS equation appears to be similar to a continuous piecewise parabola function. An intuitive answer that may emerge from the present analysis can be explained as follows. Starting from an initial random distribution the step profile first evolves to a pattern with parabolic meanders spanning with different parabola edges (preliminary instability). Once the profile develops parabolic structures there is an additional evolution of the profile. As time proceeds the amplitude of the unstable branch, the second stage of the dynamics, has different physical mechanisms which are clearly distinguished. (i) The typical behavior: the meander amplitude grows linearly with time, (ii) the amplitude disappears at a finite time, (iii) the amplitude profile decreases to 0 exponentially and (iv) nonmoving front. For situation (ii) the collapsing time is expressed exactly in term of physical parameters. Those different behaviors are found in the presence of the Mullins term which destroys the similarity structure of the CKS equation. The different scenarios are obtained by varying the initial transverse meandering amplitude, k_0, from small to large values. The typical behavior is valid for large t, provided that k_0 exceeds the critical value k_c. In this case the transverse meandering amplitude follows, for large t, the dynamics given by the simplified CKS equation. There exist numerical simulations that seem consistent with the above scenarios (see Refs. 7, 9, and 18) for different physical conditions. That is to say any physical system enjoying the same CKS equation should present the similar behaviors.

The present analytical approach should work perfectly well in the modified CSK Eq. (6). Since an identity of the type [Eq. (19)] still holds for any γ, the key ingredient in the analysis is the following explicit stationary parabolic solution having the (general) form $u_\gamma(y,t) = -\frac{1}{2}(y-\gamma)^2$. So that the initial truncated parabola, depending on γ, is given by $u_\gamma(y,0) = -\frac{1}{2}(y-\gamma)^2$, for $|y-\gamma| < k_0, k_0 > 0$ and zero elsewhere.

Arguing as above we routinely exhibit identical physical scenarios, which support the numerical simulation presented in Ref. 6. In particular, a large initial mound develops a structure with the typical behavior, while the small one disappears at a finite time. The different scenarios are preserved even if the term $\gamma\partial_y^3 u$ breaks the $y \to -y$ symmetry. For Eq. (6) the critical width is found to be $\sqrt{3}$.

Despite this, we will need to experimentally understand the dependence of the general mechanism for the meander instability on the initial transverse meandering amplitude, k_0. We believe that the preliminary results presented here are expected to motivate further theoretical and experimental-studies, even if the experiments with an imposed small initial cutoff parabolalike structure seem to be premature.

We conclude with one remark on the simplified CKS Eq. (13). Since the stationary parabola solution (16) is

also an exact stationary solution to Eq. (13), it is reasonable to expect that similar qualitative scenarios can emerge from the simplified CKS equation using an analytical approach. This question constitutes an interested line for future inquiries.

ACKNOWLEDGMENT

This work was supported by the French ANR Grant JC05-41831 and by the Conseil Régional de Picardie.

*Corresponding author; guedda@u-picardie.fr

[1] J. Villain and A. Pimpinelli, Collection Aéa-Saclay, Eyrolles, 1995.
[2] C. Misbah and O. Pierre-Louis, Phys. Rev. E **53**, R4318 (1996).
[3] Y. N. Yang, E. S. Fu, and E. D. Williams, Surf. Sci. **356**, 101 (1996).
[4] G. S. Bales and A. Zangwill, Phys. Rev. B **41**, 5500 (1990).
[5] J. Munoz-Garcia, R. Cuerno, and M. Castro, Phys. Rev. E **74**, 050103(R) (2006).
[6] F. Gillet, Z. Csahok, and C. Misbah, Phys. Rev. B **63**, 241401(R) (2001).
[7] T. Frisch and A. Verga, Phys. Rev. Lett. **96**, 166104 (2006).
[8] T. Frisch and A. Verga, Physica D **235**, 15 (2007).
[9] M. Raible, S. J. Linz, and P. Hänggi, Phys. Rev. E **62**, 1691 (2000).
[10] J. D. Weeks and W. van Saarloos, Phys. Rev. A **35**, 3001 (1987).
[11] F. Gillet, O. Pierre-Louis, and C. Misbah, Eur. Phys. J. B **18**, 519 (2000).
[12] Z. Csahók, C. Misbah, and A. Valance, Physica D **128**, 87 (1999).
[13] P. Politi and D. ben-Avraham, Physica D **238**, 156 (2009).
[14] P. Politi and J. Villain, Phys. Rev. B **54**, 5114 (1996).
[15] M. Castro, R. Cuerno, L. Vazquez, and R. Gago, Phys. Rev. Lett. **94**, 016102 (2005).
[16] M. Raible, S. J. Linz, and P. Hänggi, Phys. Rev. E **64**, 031506 (2001).
[17] T. Tiedje, K. A. Mitchell, B. Lau, A. Ballestad, and E. Nodwell, J. Geophys. Res. **111**, F02015 (2006).
[18] A. D. Verga, Phys. Rev. B **80**, 174115 (2009).